Supplementary Information

Tunable Zn^{2+} Desolvation Behavior in MnO_2 Cathode via Self-Assembled Phytic Acid Monolayers for Stable Aqueous Zn-ion Battery

Tianhang Ding[a,b,1], Shichao Yu[a,1], Ziyu Feng[a], Bin Song[c,*], Hong Zhang[d,*], and Ke Lu[a,b,*]

[a]*Institutes of Physical Science and Information Technology, School of Materials Science and Engineering, Anhui University, Hefei, Anhui 230601, China. *Email:* luke@ahu.edu.cn *(K.L.)*

[b]State Key Laboratory of Polymer Materials Engineering, Sichuan University, Chengdu, Sichuan 610065, China.

[c]*School of Chemistry and Chemical Engineering, Harbin Institute of Technology, Harbin, Heilongjiang 150001, China. *Email:* zhanghonghit@hit.edu.cn *(H.Z.)*

[d]*Institute of Functional Nano & Soft Materials (FUNSOM), Soochow University, Suzhou, Jiangsu 215123, China. *Email:* bsong@suda.edu.cn *(B.S.)*

[1]T.D. and S.Y. contributed equally to this work.

Materials synthesis

Preparation of MnO_2 nanorods: Preparation of manganese dioxide nanorods was based on a previous synthesis method.[1] The $MnSO_4 \cdot H_2O$ solution (2.028 g) and 0.5 M H_2SO_4 (8 ml) were dissolved in 300 ml deionized water and stir at room temperature, then the $KMnO_4$ solution (1.264 g, 100mL) slowly added to the solution and stirred for 2h at room temperature. The mixture was then heated at 120 ℃ for 12 h in a Teflon-lined autoclave. After the reaction, the obtained suspension was filtered and cleaned, and then vacuum-dried for 12 h.

Self-assembly preparation of MnO_2@PA nanorods: The MnO_2@PA nanorods was prepared through a facile interfacial self-assembly process similar to our previous work with more controlled synthesis method.[2] Typically, 20 μL of phytic acid (0.7 wt%) was added into 50 mL of the manganese oxide colloidal suspension (0.3 g) under vigorous stirring at 2h. Then, stopped stirring and let stand for 24h waiting the self-assembly process. The mixture was filtered and rinsed with water thoroughly. The obtained wet powders were then dried at 80 °C in the vacuum oven to obtain the final MnO_2@PA nanorods.

Materials characterization

The X-ray diffraction (XRD) measurements in this study were conducted using a Rigaku DMAX 2500 instrument that is equipped with a Cu Kα X-ray tube. The microstructure of samples were analyzed by transmission electron microscopy (TEM, JEM-2100F). The elemental mapping was performed using the energy dispersion spectroscopy (EDS) connected to the TEM instrument. The ESCALAB 250 X-ray photoelectron spectrometer was utilized to capture the X-ray photoelectron spectra (XPS). FTIR spectra of MnO_2 and modified MnO_2 cathodes were acquired in the range 960-1010 cm^{-1} using a PerkinElmer Frontier FTIR spectrometer (PerkinElmer, Boston, MA, USA). The chemical bonds of MnO_2 and modified MnO_2 cathodes were characterized by LabRAM HR Evolution microconfocal Raman spectrometer (HORIBA Jobin Yvon, France). The pH meter has been applied to the monitoring of the pH of electrolyte in real-time during an exercise period.

Electrochemical measurements

The as-prepared powder, acetylene black, and polyvinylidene difluoride (PVDF) binder were mixed using N-methylpyrrolidone (NMP) as the dispersant at a mass ratio of 7:2:1 and formed a homogeneous slurry, then evenly coated to the hydrophilic carbon paper. Then the working electrode was perforated into discs with a diameter of 12 mm and the mass loading of each cathode was 1-2 mg cm^{-2}. Thereafter, coin cells (CR 2016) were assembled with metallic Zn as anode, nonwoven filter paper as the separator, aqueous 2 M $ZnSO_4$ was used as electrolyte. The batteries charge/discharge and galvanostatic intermittent titration technique (GITT) was carried out on Neware CT-4008 analyzers and the voltage range form 0.8 to 1.8 V at different current densities. And electrochemical impedance spectroscopy (EIS) tests and cyclic voltammetry (CV) were carried out by a Germy electrochemical workstation. The differential capacitance curve was calculated from the equation: $C = -(\omega Z_{im})^{-1}$, where C is the differential capacitance and ω is the angular frequency, Z_{im} is the imaginary part of the impedance, and 1000 Hz was selected as the specific frequency.

Galvanostatic Intermittent Titration Technique (GITT)

In the GITT analysis, the potential window for the cycling test of a coin-cell at 100 mA g^{-1} was 0.8-1.8 V vs. Zn/Zn^{2+}. Constant current is applied for 5 min each pulse, and then the battery is rest for 2 h. The value of the apparent chemical diffusion coefficient can be obtained by the following formula:

$$D(GITT) = \frac{4}{\pi\tau}\left(\frac{m_B}{\rho_B S}\right)^2\left(\frac{\Delta E_s}{\Delta E_\tau}\right)^2$$

Where τ is the resting time, m_B is the mass of the active substance, S is the area of electrode sheet, ΔE_s is the change of quasi-equilibrium potential of battery, ΔE_t is the potential change during constant current, and ρ_B is the molar volume 5.02 g cm^{-3}.

Analysis using the Randles-Sevcik relationship

According to the of $I_p = (2.69 \times 10^5)\, n^{1.5}\, S\, D^{0.5}\, C\, v^{0.5}$, where I_p is the peak current, n is the charge transfer number[3], S is the geometric area of the active electrode, D is the ion diffusion coefficient, C is the concentration of ions in the cathode, and v is the potential scan rate. The n, S, and C are constant in our battery system. The slope of the curve ($I_p \sim v^{0.5}$) was used to estimate ions diffusion rate[4].

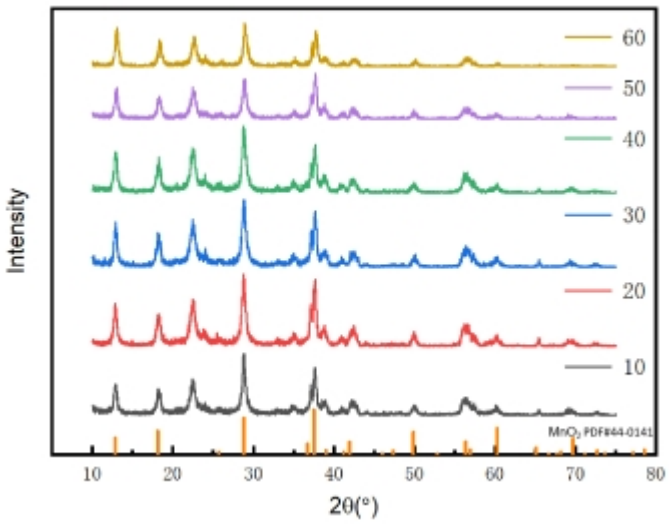

Figure S1. XRD patterns of MnO2@PA at different phytic acid concentrations.

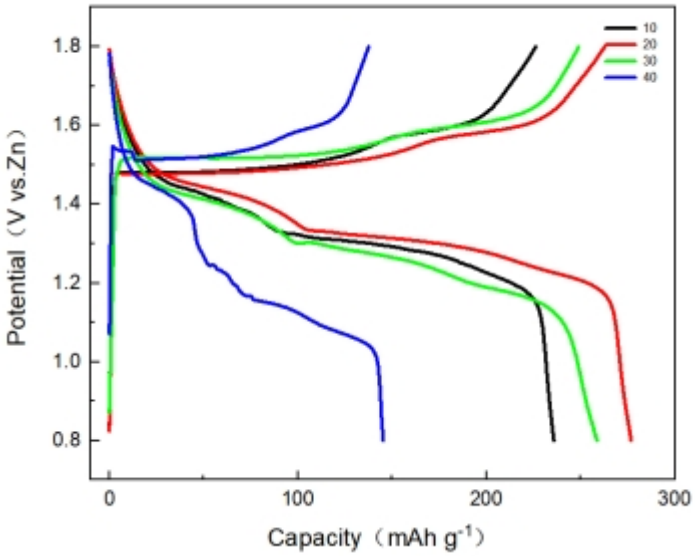

Figure S2. Charge-discharge curves of MnO2@PA at different phytic acid concentrations.

Previous studies have shown that PA, as a strong acid, has an etching effect on manganese dioxide, so we conducted a series of experiments on the dosage of PA. The XRD spectroscopy was utilized to examine whether the lattice structure of manganese dioxide nanorods was disrupted or not, as shown in Figure S1. Obviously, the intensity of the characteristic peaks was slightly attenuated with the increase of PA dosage. Then we selected the samples with 10, 20, 30, and 40 μL PA dosage with clear characteristic peaks for electrochemical testing, and the results are shown in Figure S2. The PA dosage of 20 μL has the highest charge/discharge capacity. Particularly, after doubling the dosage, the material showed very poor electrochemistry. So, we chose a phytic acid solution with a concentration of 0.7 wt% and a dosage of 20 μL for subsequent experiments.

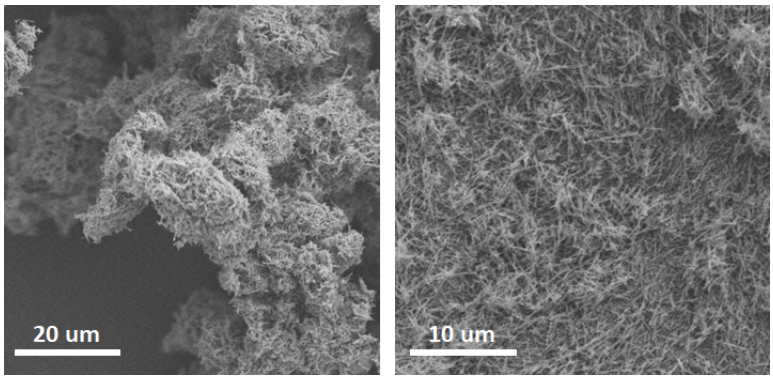

Figure S3. SEM image of MnO_2@PA

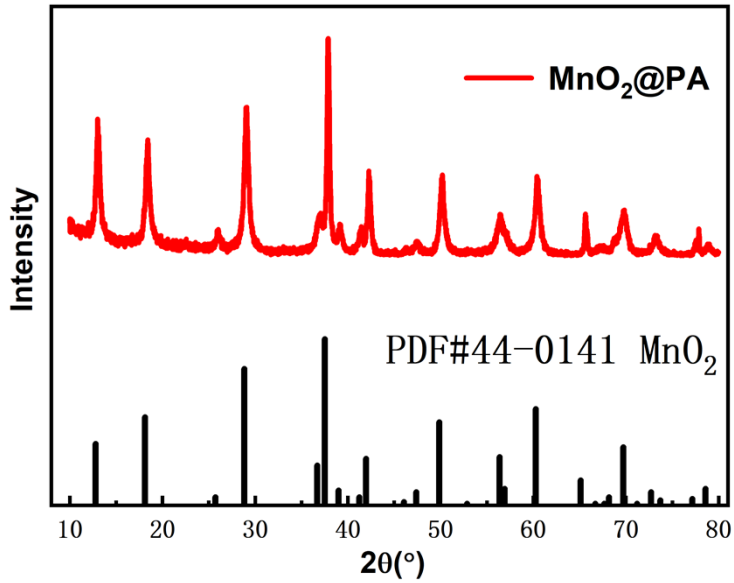

Figure S4. XRD patterns of MnO_2@PA powerd.

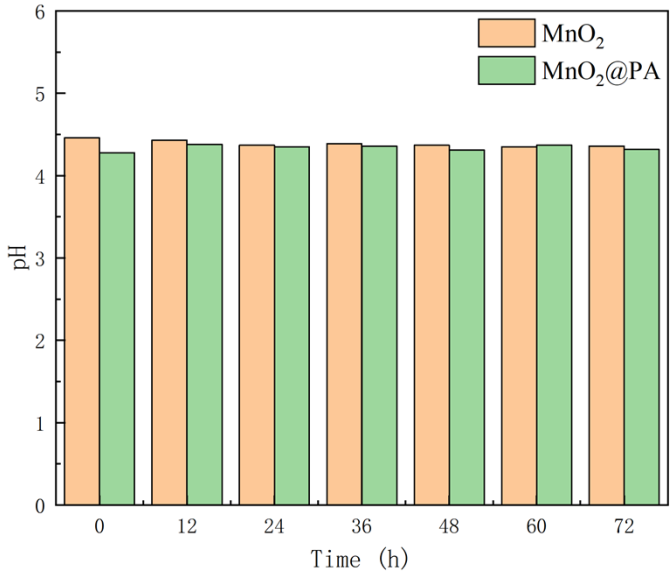

Figure S5. pH change curves of MnO_2 and MnO_2@PA cathodes immersed in 2M $ZnSO_4$ solution.

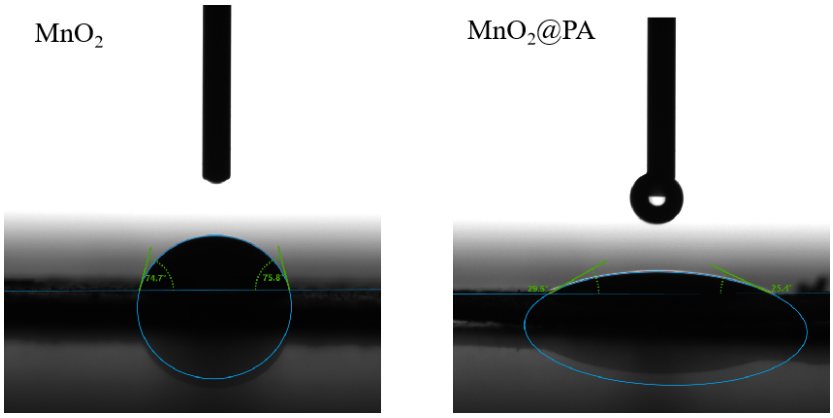

Figure S6. The contact angle tests of the different cathodes.

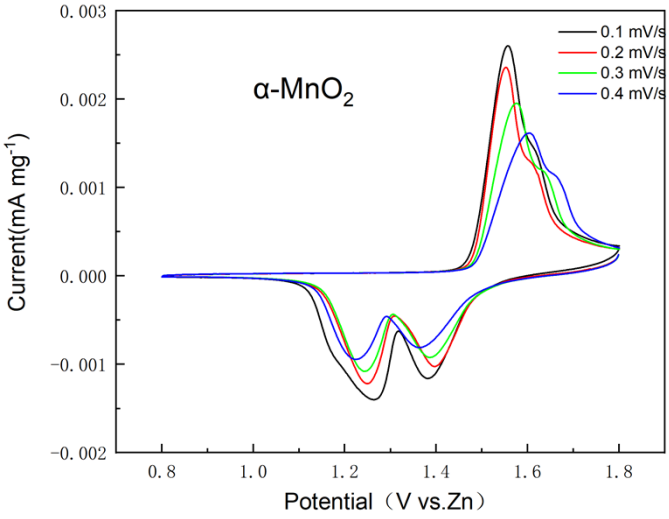

Figure S7. CV curves of MnO_2 at various sweep rates.

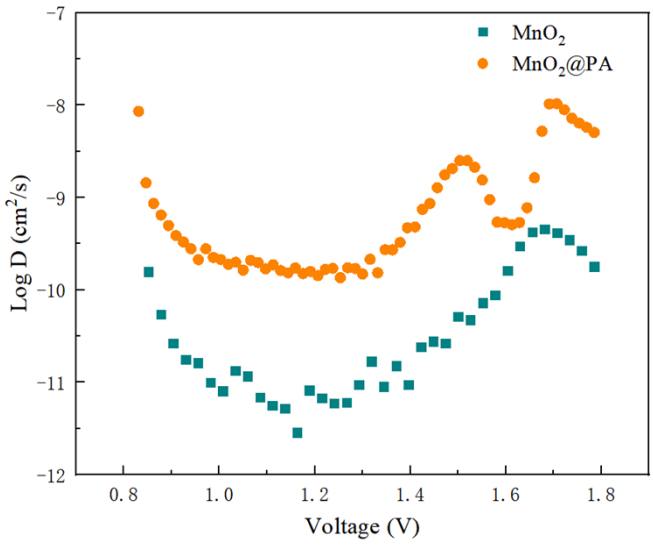

Figure S8. The ions diffusion coefficient vs. voltage for MnO_2@PA and MnO_2 during 2nd charge.

Figure S9. XRD patterns of MnO_2@PA and MnO_2 cathodes after 500 cycles.

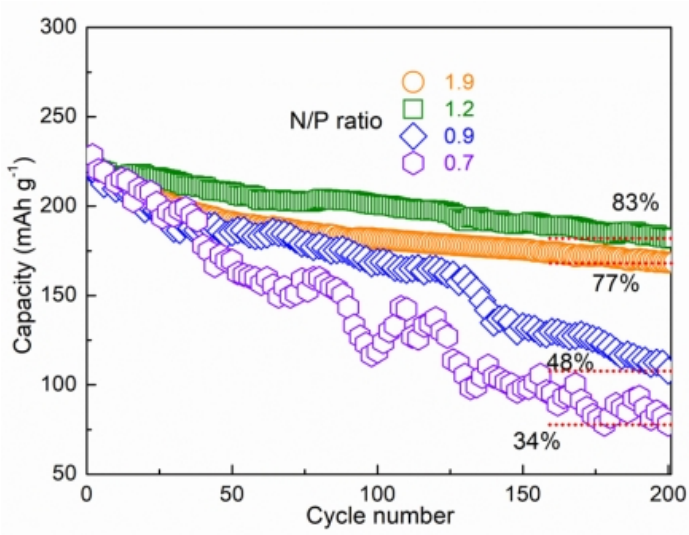

Figure S10. The comparative electrochemical performance of Zn-MnO_2@PA cells with different N/P ratios.

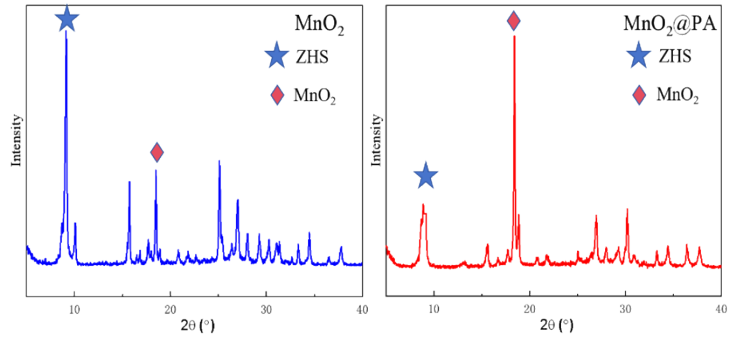

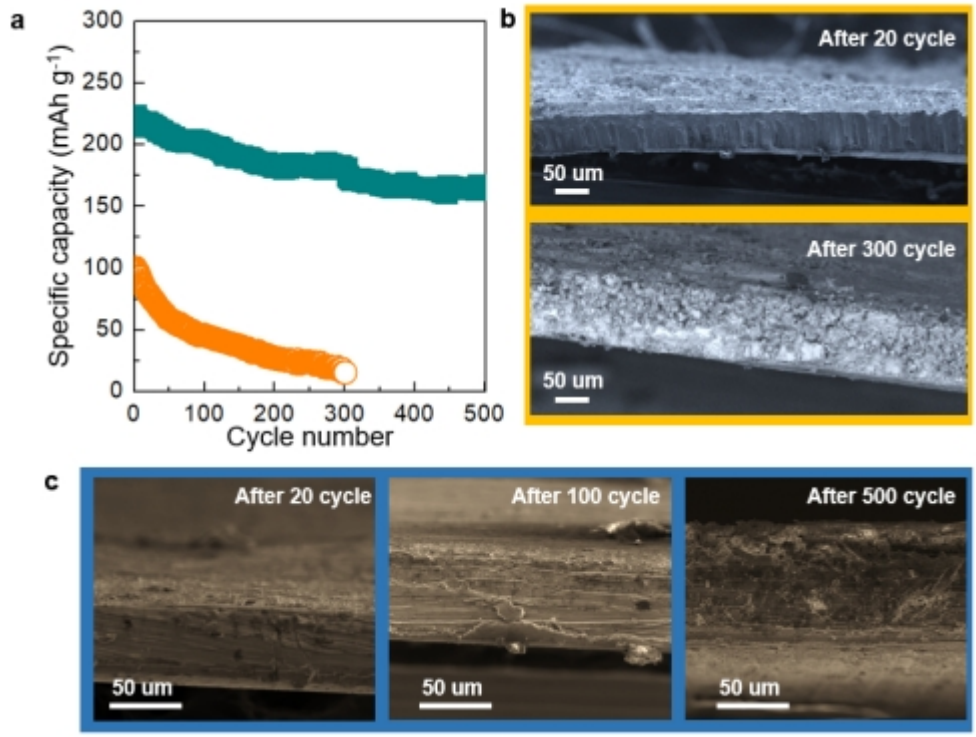

Figure S11. (a) This study examines the cycling performance of pristine Zn-MnO_2 and modified Zn-MnO_2@PA cells. Scanning electron microscope cross-sectional image of (b) the Zn-MnO2 cell anode and (c) modified Zn-MnO_2@PA cell anode following the completion of the cycling process are presented herewith.

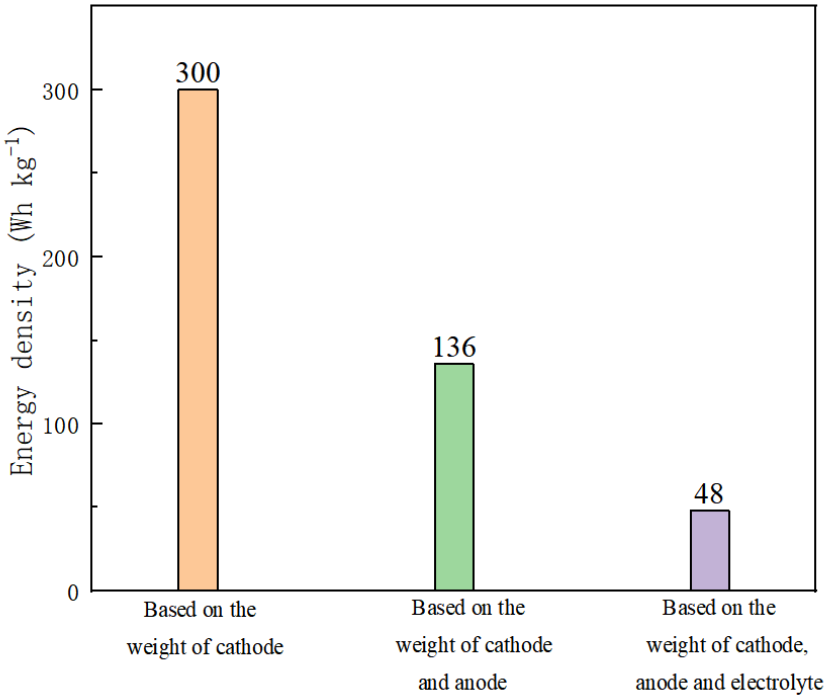

Figure S12. The calculated energy densities of Zn-MnO_2 full batteries, where the influence of the weight of cathode, anode and electrolyte on the calculation was considered.

Table S1. The Inductively Coupled Plasma Mass Spectrometry (ICP-MS) results of the beaker cells assembled with different cathodes after the cycling test.

Samples	P (ppm)	Mn (ppm)
Fresh MnO_2	0	0
Fresh MnO_2@PA	0.1	0
MnO_2 after 200 cycles	0	9.57
MnO_2@PA after 500 cycles	1.2	0.7

The structure of the coating layer is further verified by the Inductively Coupled Plasma Mass Spectrometry (ICP-MS) analyses. Considering that the amount of electrolyte used in coin batteries makes it difficult to support ICP-MS testing, beaker batteries were used for experimental testing. Therefore, we first immersed the positive and negative electrodes in the electrolyte system without charging and discharging tests to verify the stability of the phytate layer. The results are shown in Table S1, after 24 hours of immersion, very few P-element signals are detected in the solution, which proves that the phytic acid layer is well adsorbed on the MnO_2 substrate and basically does not dissolve in the electrolyte. We then carried out charge/discharge tests and tested the electrolyte after cycling. In the post-cycling Zn-MnO_2 beaker battery electrolyte, obvious Mn elements can be observed, indicating that the electrode material will be partially dissolved during the battery cycling process to seriously affect its performance. In contrast, no significant amount of P and Mn elements were examined in the post-cycling Zn-MnO_2@PA beaker cell, which well reveals the protective effect of the phytic acid layer.

Table S2. A comparison of the electrochemical performance with other reported results

Cathode	Capacity (mAh g^{-1})/current (mA g^{-1})	Capacity retention (%)/cycles	Electrolyte system	Ref.
MnO_2@PA	272/10	73/500	2M $ZnSO_4$	This work
MnO_2@MnHCF-PPy	263/15	87/200	2M $ZnSO_4$	[1]
BPA@MnO_2	210/28	62/400	1M $ZnSO_4$	[2]
α-MnO_2/rGO-PPy	248.8/50	85.9/100	3M $Zn(CF_3SO_3)_2$	[5]
δ-MnO_2	243/10	89.5/500	H_2O, DMC and 2M $Zn(OTf)_2$	[6]
Co_xMnO_2	235.3/10	88.1/10000	2M $ZnSO_4$ and 0.2M $MnSO_4$	[7]
CNT/MnO_2-PPy	253.9/10	87.4/1000	2M $ZnSO_4$ and 0.1M $MnSO_4$	[8]
α-MnO_2@PPy	148/100	57.4/100	1M $ZnSO_4$ and 0.1M $MnSO_4$	[9]
α-MnO_2@δ-MnO_2	153.8/20	98.1/1000	6M KOH	[10]
MnBirMO	256/10	97/8000	2M $ZnSO_4$ and 0.1M $MnSO_4$	[11]
V_2O_5/rGO	175/10	77.3/200	3M $ZnSO_4$	[12]
MnO_2@AEPA	223/50	97/1700	2M $ZnSO_4$ and 0.1M $MnSO_4$	[13]
MnOF0.04	249.1/20	76.2/3500	2M $ZnSO_4$ and 0.2M $MnSO_4$	[14]
β -MnO_2/SATP	218.4/2000	43.2/500	2M $ZnSO_4$ and 0.5M $MnSO_4$	[15]
CrNi-MnO_2	586/20	44.1/1600	2M $ZnSO_4$ and 0.1M $MnSO_4$	[16]

Reference

[1] Z. Shang, H. Zhang, M. Wang, Q. Chen, K. Lu, *Nanoscale* **2022**, *14*, 6085-6093.

[2] S. Gao, B. Li, K. Lu, S. Alabidun, F. Xia, C. Nickel, T. Xu, Y. Cheng, *Acs Applied Materials & Interfaces* **2021**, *13*, 23724-23731.

[3] P. Li, L. Y. Shao, P. F. Wang, H. X. Yu, S. S. Qian, M. Shui, N. B. Long, J. Shu, *Electrochimica Acta* **2015**, *180*, 120-128.

[4] G. M. Zhou, H. Z. Tian, Y. Jin, X. Y. Tao, B. F. Liu, R. F. Zhang, Z. W. Seh, D. Zhuo, Y. Y. Liu, J. Sun, J. Zhao, C. X. Zu, D. S. Wu, Q. F. Zhang, Y. Cui, *Proceedings of the National Academy of Sciences of the United States of America* **2017**, *114*, 840-845.

[5] T. Niu, J. Li, Y. Qi, X. Huang, Y. Ren, *Journal of Materials Science* **2021**, *56*, 16582-16590.

[6] Y. Dong, L. Miao, G. Ma, S. Di, Y. Wang, L. Wang, J. Xu, N. Zhang, *Chemical Science* **2021**, *12*, 5843-5852.

[7] Q. Chen, X. Lou, Y. Yuan, K. You, C. Li, C. Jiang, Y. Zeng, S. Zhou, J. Zhang, G. Hou, J. Lu, Y. Tang, *Advanced Materials* **2023**, *35*.

[8] Y. Zhang, G. Xu, X. Liu, X. Wei, J. Cao, L. Yang, *Chemelectrochem* **2020**, *7*, 2762-2770.

[9] C. Guo, S. Tian, B. Chen, H. Liu, J. Li, *Materials Letters* **2020**, *262*.

[10] Z. Ma, G. Shao, Y. Fan, G. Wang, J. Song, D. Shen, *Acs Applied Materials & Interfaces* **2016**, *8*, 9050-9058.

[11] J. Ding, H. Du, G. Cai, S. Huang, C. Peng, L. Wang, J. Luo, X. Wang, M. Xue, X. Zhang, J. Sun, J. Chen, *Nano Energy* **2023**, *112*.

[12] S. Wang, K. Zhu, L. Yang, H. Li, S. Wang, S. Tang, M. Zhang, A. Abliz, F. Zhao, *Ionics* **2020**, *26*, 5607-5615.

[13] X. Xiao, L. Zhang, W. Xin, M. Yang, Y. Geng, M. Niu, H. Zhang, Z. Zhu, *Small* **2024**, *20*, 2309271.

[14] L. Ding, L. Wang, J. Gao, T. Yan, H. Li, J. Mao, F. Song, S. Fedotov, L.-Y. Chang, N. Li, Y. Su, T. Liu, L. Zhang, *Advanced Functional Materials* **2023**, *33*.

[15] M. Chen, W. Liu, D. Ren, Y. An, C. Shu, S. Zhang, W. Liang, J. Sun, F. Kang, F. Jiang, *Advanced Functional Materials* **2024**, 2404983.

[16] Y. Zhao, X. Xia, Q. Li, Y. Wang, Y. Fan, Y. Zhao, W. Liu, X. Sun, *Energy Storage Materials* **2024**, *67*, 103268.